Acta Mechanica Solida Sinica, Vol. 21, No. 3, June, 2008 ISSN 0894-9166
Published by AMSS Press, Wuhan, China. DOI: 10.1007/s10338-008-0822-5

SIMULATIONS OF MECHANICAL BEHAVIOR OF POLYCRYSTALLINE COPPER WITH NANO-TWINS **

Bo Wu Yueguang Wei*[1]

(*State-Key Laboratory of Nonlinear Mechanics, Institute of Mechanics, Chinese Academy of Sciences, Beijing* 100190*, China*)

Received 29 February 2008, revision received 3 June 2008

ABSTRACT Mechanical behavior and microstructure evolution of polycrystalline copper with nano-twins were investigated in the present work by finite element simulations. The fracture of grain boundaries are described by a cohesive interface constitutive model based on the strain gradient plasticity theory. A systematic study of the strength and ductility for different grain sizes and twin lamellae distributions is performed. The results show that the material strength and ductility strongly depend on the grain size and the distribution of twin lamellae microstructures in the polycrystalline copper.

KEY WORDS nanocrystalline twinned copper, mechanical behavior, cohesive model, finite element simulation

I. INTRODUCTION

An electro-deposited polycrystalline copper film with nano-scale twins (or nanocrystalline twinned (NCT) copper) was synthesized with an ultra-high tensile strength. By observing the microstructures of the NCT copper using the transmission electron microscopy (TEM), one found that the material microstructures could be further subdivided into the twin/matrix lamellar substructures with high density of twin boundaries (TBs)[1]. Recently, there have been many researches on the deformation mechanism of the electro-deposited Cu with twin/matrix lamellar microstructure[1–4]. The previous researches have shown that twin/matrix lamellar microstructure of the Cu grain directly affects materials mechanical properties. Specifically, the twin boundary spacing (or the twin lamellar spacing) plays an important role in the plastic deformation and work hardening of materials.

Twin boundaries, a special kind of coherent boundary with low energy, may serve as barriers to dislocation motion and an intrinsic strengthening mechanism of ultrafine crystalline (UFC) materials. It is worth noting that the presence of twin boundaries enhances the corrosion resistance and reduces the propensity for intragranular fracture. The intergranular fracture is a main failure mechanism of the NCT copper. Recent molecular dynamics (MD) simulations on the dislocations interacting with coherent twin boundary[5,6] have shown the relatively high ductility of NCT copper to the hardening of TBs as they gradually lose coherency during plastic deformation. MD simulation is powerful in understanding the deformation mechanism of nanocrystalline metals. However, due to the limitations in time and space, it is impractical to compare the MD simulations with the experimental results. So the finite element simulations have been considered by Dao et al.[7]. A twin boundary affected

* Corresponding author. E-mail: ywei@lnm.imech.ac.cn

** Project supported by the National Natural Science Foundation of China (Nos. 10432050, 10428207, 10672163 and 10721202) and by the Chinese Academy of Science through Grant KJCX-YW-M04.

zone (TBAZ) model motivated by the grain boundary affected zone (GBAZ) model[8,9] was proposed and a comprehensive computational analysis of the deformation of ultrafine crystalline pure copper with nanoscale twins was carried out. However, high resolution TEM images of grain boundaries in electrodeposited nanocrystalline Ni and Cu show that the crystallinity of grains is maintained well up to the boundary and no second phase is observed[10]. It is very difficult to assign a different material phase to the GB zone and especially TB zone. Recently, the conventional continuum mechanics theory cannot characterize the size effects of materials in nanoscale. In recent work of Han and Gao et al., they proposed a theory based on strain gradient crystal plasticity (MSG-CP)[11,12]. Although this theory can well model the effect of inherent anisotropy of a crystal lattice on size-dependent non-uniform plastic deformation at micron and submicron length scales, there are so many parameters for each slip system that must be considered. On the other hand, it is more difficult to implement this theory by means of finite element method.

So in the present research, an isotropic assumption is adopted and a new model of polycrystalline copper with nano-scale twins is presented. The concept of twin lamellae strengthening zone is proposed and a cohesive interface model is used to simulate the phenomena of grain-boundary sliding and separation. The conventional theory of mechanism-based strain gradient plasticity (CMSG)[13] established from the Taylor dislocation model is used to simulate the strengthening mechanical behaviors and size effects of the NCT copper with the twin/matrix lamellar microstructure. Through the analysis, the fracture processes of cracks along grain boundaries of the NCT copper and the influences of intergranular fracture ductility with different grain sizes, material parameters, and the distribution of twin/matrix lamellae microstructures will be discussed. Finally, the FEM results will be compared with several experimental results.

II. CONSTITUTIVE LAWS AND CALCULATION MODEL

2.1. The CMSG Constitutive Law for Twin/Matrix Lamellae

At the nano-scale, due to the grain size effect, the mechanical behaviors of the NCT copper cannot be well described by the conventional elastic-plastic theory. So in the present research, the theory of mechanism-based strain gradient plasticity (CMSG) theory presented by Huang et al.[13,14] will be used. Here a brief description of the CMSG constitutive relations and the corresponding finite element analysis is provided.

Based on the Taylor dislocation model, the CMSG constitutive relations have been developed. For small dislocation density, Taylor dislocation model gives the shear flow stress τ in terms of the dislocation density ρ by

$$\tau = \alpha\mu b\sqrt{\rho} = \alpha\mu b\sqrt{\rho_S + \rho_G}, \tag{1}$$

where μ is the shear modulus; b is the Burgers vector; α is an empirical coefficient around 0.3 depending on the material structures and characteristics. ρ_S and ρ_G are densities of statistically stored dislocations (SSD) and geometrically necessary dislocations (GND), respectively. The GND density ρ_G is related to the effective plastic strain gradient η^p by

$$\rho_G = \bar{r}\frac{\eta^p}{b} \tag{2}$$

where $\bar{r}$ is the Nye-factor to reflect the effect of crystallography on the distribution of GNDs and is around 1.90 for face-centered-cubic (FCC) polycrystals. While η^p is effective plastic strain gradient.

The tensile flow stress σ_{flow} is related to the shear stress τ by

$$\sigma_{\text{flow}} = M\tau = M\alpha\mu b\sqrt{\rho_S + \bar{r}\frac{\eta^p}{b}} \tag{3}$$

where M is Taylor factor which acts as an isotropic interpretation of the crystalline anisotropy at the continuum level, and M is about 3.06 for FCC metals. When the effective plastic strain gradient η^p vanishes, the flow stress can be degenerated to $\sigma_{\text{flow}} = \sigma_Y f(\varepsilon^p)$ in uniaxial tension, and then the SSD density ρ_S is determined from Eq.(3) as

$$\rho_S = \left[\frac{\sigma_Y f(\varepsilon^p)}{M\alpha\mu b}\right]^2 \tag{4}$$

So the flow stress accounting for the nonuniform plastic deformation becomes

$$\sigma_{\text{flow}} = \sqrt{\left[\sigma_Y f(\varepsilon^p)\right]^2 + M^2\alpha^2\overline{r}\mu^2 b\eta^p} = \sigma_Y\sqrt{f^2(\varepsilon^p) + l\eta^p} \tag{5}$$

where

$$l = M^2\bar{r}\alpha^2\left(\frac{\mu}{\sigma_Y}\right)^2 b \approx 18\alpha^2\left(\frac{\mu}{\sigma_Y}\right)^2 b, \quad f(\varepsilon^p) = \left(1 + \frac{E\varepsilon^p}{\sigma_Y}\right)^N \tag{6}$$

is the intrinsic material length in strain gradient plasticity, σ_Y is the initial yield stress, and N is the plastic work hardening exponent ($0 \le N < 1$).

Huang et al. demonstrated that the power law visco-plastic model incorporating the strain gradient effects can be applicable to conventional power-law hardening if the rate-sensitivity exponent m is large ($m \ge 20$). Then the plastic strain rate is expressed as

$$\dot{\varepsilon}^p = \dot{\varepsilon}\left[\frac{\sigma_e}{\sigma_Y\sqrt{f^2(\varepsilon^p) + l\eta^p}}\right]^m \tag{7}$$

where $\dot{\varepsilon} = \sqrt{2\dot{\varepsilon}'_{ij}\dot{\varepsilon}'_{ij}/3}$ is the effective strain rate and $\dot{\varepsilon}'_{ij}$ is the deviatoric strain rate.

The constitutive relations in CMSG theory, which involve the conventional stress and strain only, can be expressed as given the stress-rate $\dot{\sigma}_{ij}$ in terms of the strain-rate as follows

$$\dot{\sigma}_{ij} = K\dot{\varepsilon}_{kk}\delta_{ij} + 2\mu\left\{\dot{\varepsilon}'_{ij} - \frac{3\dot{\varepsilon}}{2\sigma_e}\left[\frac{\sigma_e}{\sigma_Y\sqrt{f^2(\varepsilon^p) + l\eta^p}}\right]^m \sigma'_{ij}\right\} \tag{8}$$

where K is the bulk elastic modulus, $\dot{\varepsilon}'_{ij}$ is the deviatoric strain rate, $\sigma_e = \sqrt{3\sigma'_{ij}\sigma'_{ij}/2}$ is the effective Von Mises stress, $\dot{\varepsilon}_{kk}$ is the bulk strain rate, and δ_{ij} is the Kronecker delta tensor. The effective plastic strain gradient η^p in CMSG theory is defined in the same way as that in the higher-order MSG theory[15], and is given by

$$\eta^p = \int \dot{\eta}^p \mathrm{d}t, \quad \dot{\eta}^p = \sqrt{\frac{1}{4}\dot{\eta}^p_{ijk}\dot{\eta}^p_{ijk}}, \quad \dot{\eta}^p_{ijk} = \dot{\varepsilon}^p_{ik,j} + \dot{\varepsilon}^p_{jk,i} - \dot{\varepsilon}^p_{ij,k} \tag{9}$$

where $\dot{\varepsilon}^p_{ij}$ is the tensor of plastic strain rate.

Generally speaking, when the strain gradient effect is considered, the conventional finite element method fails. However the CMSG theory is a lower-order theory which does not involve the higher-order stress such that the governing equations are essentially the same as those in the classical plasticity. One can easily modify the existing finite element program to incorporate the plastic strain gradient effect[14, 16]. In the present research, we have implemented a C^0 three-dimensional solid element incorporating the CMSG theory in the ABAQUS finite element program[17] via its User-Material subroutine UMAT.

2.2. Simplified Model of the NCT Copper Structure

Figure 1(a) shows a bright field TEM image of an as-deposited NCT copper sample. It shows that the TBs separate grains into nano-meter thick twin/matrix lamellar structures. The thickness of twin lamellar geometry varies from about 20 nm to 1 μm, and the most grains in the Cu sample with nano-scale growth twins are equiaxed in three dimensions[2]. The post-deformation microstructure observations indicate that the plastic deformation inside the NCT copper is extremely incompatible with the TBs appearance. In order to accommodate the incompatible plastic deformation, the geometrically necessary dislocations which are related to plastic strain gradient in Eq.(2) accumulate near the TBs and cause hardening. When the matrix lamellae are thick, dislocation pile-ups form a certain stress concentration at TBs and a low applied stress is needed to activate the slip transmission of the TBs, while the high external stress is needed when the twin lamellae are thick. All these suggest that some mechanical constitutive parameters (such as the initial yield stress, the plastic strain hardening exponent, etc.) for the twin lamellae and matrix lamellae should be varied with different lamellar spacing. We assume that the material parameters of twin lamellar microstructures are different from the matrix lamellae and the thinner twin lamellae are taken as the strengthening zones which have a strengthening effect on the whole deformation of the electro-deposited polycrystalline Cu with twin/matrix lamellar microstructure. Otherwise, the hardening effects of TBs can be characterized by treating TBs with an internal interface and causing strong strain gradient strength for incompatible plastic deformation of two different material lamellae (twin/matrix lamellae).

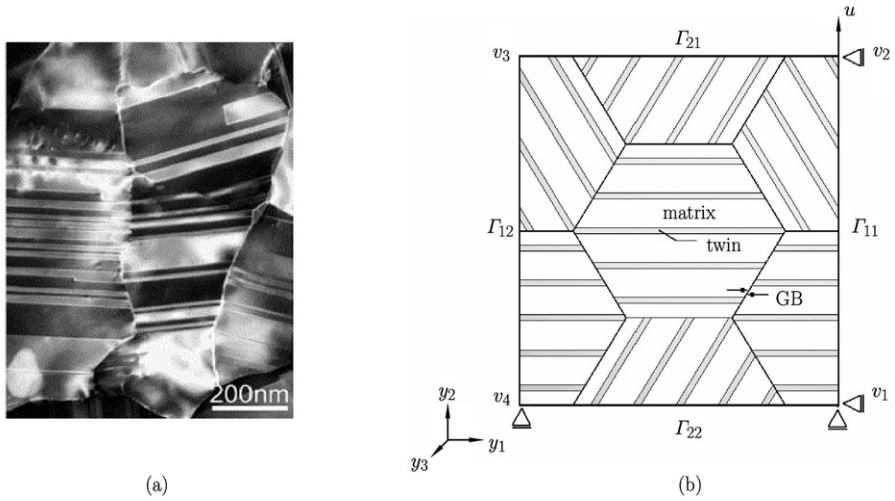

Fig. 1. (a) Bright field TEM image of Cu with nano-scale twins(figure reproduced from Ref.[2]) and (b) Schematic drawing of calculation model and boundary conditions.

2.3. The Cohesive Model Used in Grain Boundary

Cohesive interface model was presented by Barenblatt[18] and Dugdale[19] more than 40 years ago. In recent years, numerous cohesive interface model formulations have been widely used to simulate fracture initiation and propagation[20–22]. Molecular dynamics simulations and direct experimental evidences have indicated that the roles of grain boundary sliding and separation are more important with smaller grain size[23–25]. In the present numerical study, the cohesive models are used to describe the initiation and evolution of intergranular cracks without arbitrarily introducing initial cracks after the normal or shear traction or a combined traction across the interface. Then actual cracks naturally form and grow due to the heterogeneous stress/strain field which is caused by the geometry structures and variations in materials properties. To describe the evolution of damage under a combination of normal and shear deformation across the interface, it is useful to introduce an effective displacement defined as $\delta_m = \sqrt{\langle\delta_n\rangle^2 + \delta_s^2 + \delta_t^2}$. The $\langle\rangle$ represents the Macaulay bracket, which is used to emphasize that a pure compressive deformation does not initiate damage. δ_n, δ_s and δ_t represent the relative displacements when the deformation which is either purely normal to the interface or only in the first or the second shear direction respectively. The traction-separation behavior of cohesive constitutive model is indicated as in Fig.2. Let T_1 and λ_1 ($\lambda_1 = \delta_m^0/\delta_m^f$) be the critical values of traction and dimensionless displacement, respectively. Here T is the traction, δ_m^0 is the critical separation effective displacement at damage initiation, δ_m^f is separation effective displacement at complete failure and K_c is the initial separation stiffness of the cohesive element.

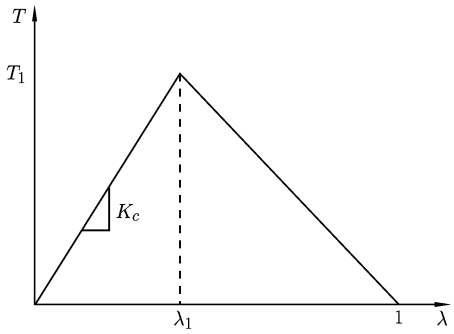

Fig. 2 Cohesive force curve of cohesive model.

2.4. Finite Element Calculation Model and Boundary Conditions

A quasi-three-dimensional representative volume element which taking into account of three dimensional effects is presented here. Figure 1(b) shows the schematic drawing of representative calculation model, where each grain contains five twin lamellae in different orientations. The representative calculation model consists of seven idealized hexagon grain, and the radius R of grain is the radius of circumcircle of hexagon. As displayed in Fig.1(b), the gray zones stand for the twin lamella strengthening zones with thickness D_T, while the white zones stand for the matrix lamella with thickness D_M. The cohesive interface layers with zero thickness model grain boundaries are between two hexagon grains. Here the finite element mesh includes eight-node, iso-parametric element C3D8 which is based

on the CMSG constitutive relations via UMAT of ABAQUS and cohesive element Coh3D8 (available in ABAQUS). Periodic assumption is used to simplify the calculation model, where the orientation of the twin lamellae in whole grains is considered as periodic distribution. Periodic boundary conditions are enforced along the four sides in y_1y_2 coordinate plane[26]:

$$\bar{\boldsymbol{u}}_{12} - \bar{\boldsymbol{u}}_{v_4} = \bar{\boldsymbol{u}}_{11} - \bar{\boldsymbol{u}}_{v_1} \tag{10}$$

$$\bar{\boldsymbol{u}}_{22} - \bar{\boldsymbol{u}}_{v_1} = \bar{\boldsymbol{u}}_{21} - \bar{\boldsymbol{u}}_{v_2} \tag{11}$$

$$\bar{\boldsymbol{u}}_{v_3} - \bar{\boldsymbol{u}}_{v_2} = \bar{\boldsymbol{u}}_{v_4} - \bar{\boldsymbol{u}}_{v_1} \tag{12}$$

Here, $\bar{\boldsymbol{u}}_{ij}$ is the displacement vector for any point on the corresponding boundary Γ_{ij}, and $\bar{\boldsymbol{u}}_{v_i}$ the displacement vector for each vertex v_i. Rigid body motions can be eliminated by requiring that $\bar{\boldsymbol{u}}_{v_k} = 0$, for either $k \in \{1, 2, 4\}$. Otherwise, a displacement boundary condition $\bar{\boldsymbol{u}}_Z$ which considers the third dimensional effect is enforced in the y_3 coordinate direction perpendicular to y_1y_2 coordinate plane, assuming that the material geometry in the z-direction is also a periodic structure which has a finite-thickness.

III. RESULTS AND DISCUSSION

3.1. Intergranular Fracture Affected by Twin Lamellae Microstructures

In the present analysis, a comparative study of the intergranular fracture ductility with different grain sizes and twin/matrix lamellae material parameter is performed. For convenience, the twin lamellar intrinsic material length l_T and the twin lamellar initial yield stress σ_{yT} are taken as the normalizing quantities to normalize parameters of NCT copper with length dimensions and with stress dimensions, respectively. The overall stress-strain relation with parameter dependence can be expressed as follows

$$\frac{\sigma}{\sigma_{yT}} = F\left(\frac{R}{l_T}, \frac{D_T}{l_T}, \frac{D_M}{l_T}; \frac{E_T}{\sigma_{yT}}, \frac{K_c}{\sigma_{yT}}, \nu_T, N_T, m_T, \frac{E_M}{\sigma_{yT}}, \nu_M, \frac{\sigma_{yM}}{\sigma_{yT}}, N_M, m_M; \frac{l_M}{l_T}; \varepsilon\right) \tag{13}$$

where the subscript T and M indicate twin and matrix, respectively. There are many parameters included in Eq.(13). For simplification, in most cases of the present study we consider the material parameters $E_M = E_T = 166.66\sigma_{yT}$, $\nu_M = \nu_T = 0.3$, $m_T = m_M = 20$,$N_T = N_M = 0.2$, $\sigma_{yT}/\sigma_{yM} = 2$ and $K_c = 166.66\sigma_{yT}$. And assume that these material parameters will not change with twin/matrix lamellae geometry size. Two different length scale (grain size $R/l_T = 0.5$ and $R/l_T = 5$) with the same twin lamellar volume fraction are considered under axial tensile loading conditions, assuming that both thicknesses of twin lamella D_T and matrix lamella D_M are kept the same proportion to grain radius R in different calculation cases.

The dependence on the ratios of initial yield stress of the matrix to that of twin lamellae of NCT copper with different grain sizes is shown in Fig.3, when the parameters of cohesive interface are fixed. As shown in Fig.3, the strength and global ductility of NCT copper are sensitive to the ratios. With

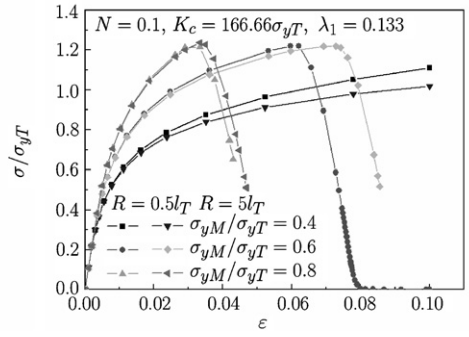

Fig. 3. The dependence of the stress-strain relations on different ratios (σ_{yM}/σ_{yT}) of initial yield stresses of matrix and twin lamellae with different sizes (R/l_T) of representative volume element.

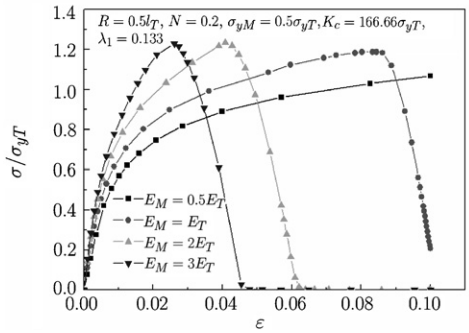

Fig. 4. The dependence of the stress-strain relations on different elastic moduli (E_M) of matrix lamellae with grain size ($R/l_T = 0.5$).

the increasing initial yield stress of matrix lamella, the strength of material is increased greatly but the global ductility will be decreased when other material parameters fixed. And it is helpful to delay the intergranular fracture by increasing the difference of initial yield stresses between matrix and twin lamellae. Furthermore, with decreasing the difference, the dependence of intergranular fracture on the grain size is gradually diminished.

Although both the materials of twin and matrix lamellae are copper, the elastic moduli of twin/matrix lamellae are maybe different due to the elastic anisotropy of monocrystalline copper. Figure 4 shows the influence on stress-strain relations of NCT copper by varying the elastic moduli of matrix lamellae. As expected, the variation elastic moduli of matrix lamellae obviously influence the global ductility of nano-twinned copper. And with increasing elastic moduli, the intergranular fracture of polycrystalline copper with nano-scale twins is easier to take place.

Figure 5 shows that the overall ductility and strength of NCT copper are sensitive to the twin/matrix lamellar work hardening exponent. When the exponent N is small, the occurrence of intergranular fracture will be deferred greatly but the effect of work hardening is not obvious. Recent studies on the work hardening of ultrafine-grained copper with nanoscale twins[27] have indicated that the conventional work hardening mechanism by the forest dislocations for the coarse grain FCC metal is not dominant due to the thin twin lamellae structures introduced. So the improvement of global ductility of NCT copper may benefit significantly from the decreasing work hardening exponent by a new work hardening mechanism in twin/matrix lamellae structures.

Figure 6 shows the dependence of the stress-strain relations on the volume fraction V_T of twin lamellae for grain size $R/l_T = 0.5$. Three cases of the twin lamellae volume fractions (V_T = 11.5%, 18.5% and 26.0%) are considered, without changing the thicknesses of twin lamellae and other material parameters. Although the thicknesses of matrix lamellae are decreased with increasing twin lamellae volume fraction, in this present calculation, we presume that the material parameters are not altered with the thickness of matrix lamella. Namely, only the volume fraction of twin lamellae strengthen zone is considered in the example. The results show that the general strength is enhanced with the increasing volume fraction of twin lamellae, but the global ductility is decreased. The calculation results are inconsistent with the previous experimental results in which the strength and global ductility of nano-twins copper are both increased with the increase of twins density. This is because two important factors are not considered in this calculation. Firstly, the contribution to ductility of twin boundaries due to the coherency loss during plastic deformation is not taken into account due to the limit of continuum finite element simulation. Secondly, the properties of grain boundaries (i.e. the parameters of cohesive interface model) should be altered with changing geometrical microstructure of twin/matrix lamellae in grain interior.

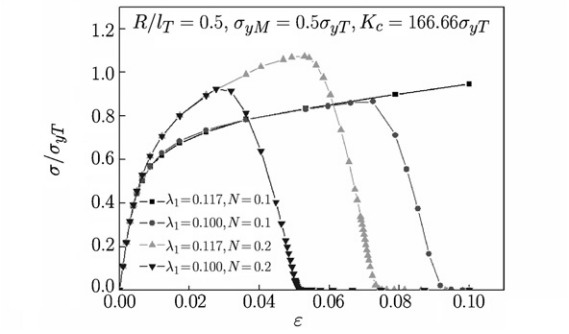

Fig. 5. The dependence of the stress-strain relations on the plastic work hardening exponents (N) of twin/matrix lamellae.

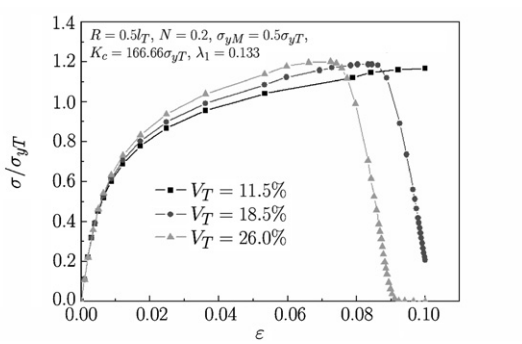

Fig. 6. The dependence of the stress-strain relations on the volume fractions (V_T) of twin lamellae.

3.2. Comparison with Experimental Results

The material parameters and the representative calculation model geometry scales of Cu with nano-scale twins in the present analysis are obtained from the experiments of Shen et al.[12]. Two different

twin lamellar spacing, nt-Cu-fine and nt-Cu-medium (nano-twined Cu with different twin densities), are considered. Since both the materials of twin lamellae and matrix lamellae are copper, we assume that some material parameters of twin lamellae and matrix lamellae are equal, such as the Young's modulus $E_T = E_M = 100$ GPa, the Poisson's ratio $\nu_T = \nu_M = 0.3$, the rate sensitivity exponent is $m_T = m_M = 20$, the Taylor factor $M_T = M_M = 3.06$, the Nye-factor $\bar{r}_T = \bar{r}_M = 1.90$, the empirical coefficient in the Taylor dislocation model $\alpha_T = \alpha_M = 0.25$, the magnitude of the copper Burgers vector $b_T = b_M = 0.271$ nm. The average grain radii of the experiment samples are both $R = 260 \pm 10$ nm. Then the radius R of grain of representative calculation model is fixed at $R = 260$ nm. As TBs block dislocation motions inside crystals, Shen et al. proposed that the initial yield stresses of twin lamellae and matrix lamellae with different lamellar spacing can be represented, analogous to the classical H-P relation[2].

$$\sigma_y = \sigma_0 + K_T \cdot l^{-n} \tag{14}$$

where σ_y is the initial yield stress, σ_0 is a reference stress, K_T is a constant, l is the mean twin lamella spacing, and n is a coefficient ranging from 0.5 to 1. All the parameters in Eq.(14) can be found in the experiment data of Shen et al. And as shown in recent studies on the work hardening of ultrafine-grained copper with nanoscale twins[27], Chen and Lu have indicated that the work hardening exponent N is decreased with the decreasing of twin lamellae thickness. So in the present numerical study, the work hardening exponents of different thickness twin lamellae are allowed to vary from 0.08 to 0.15. All the parameters of two samples with different twin/matrix lamellar spacing are list in Table 1. The maximum nominal stress criterion for damage initiation at grain boundary cohesive zone is introduced, namely the critical traction stress T_1 is pre-established. Here the separation strength of T_1 is chosen to coincide with the bulk initial yield stress of twin lamella, and the separation effective displacement $\left(\delta_m^f - \delta_m^0\right)$ is assumed to be 50 nm, the initial separation stiffness K_c of grain boundary is equal to the copper Young's modulus.

Table 1. **Summary of microstructure characteristic parameters**

Sample	D_T (nm)	D_M (nm)	σ_{yT} (MPa)	σ_{yM} (MPa)	N_T	N_M
nt-Cu-fine	12	30	950	660	0.08	0.1
nt-Cu-medium	33	61	750	550	0.1	0.15

The numerical results with different twin/matrix lamellae spacings are shown in Fig.7. From Fig.7, the stress-strain curves calculated by finite element method agree well with the experimental data in trend. Although the real failure process in electro-deposited polycrystalline copper with nano-scale growth twins is complicated, the computational model still characterizes the experimentally observed failure trend of nano-twins copper to a certain extent.

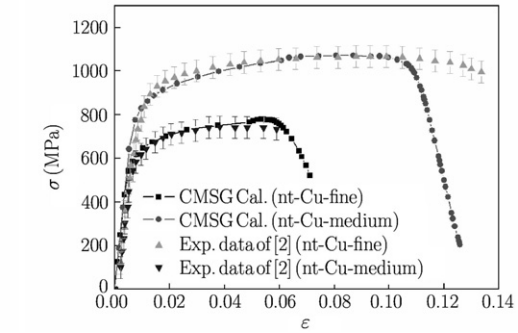

Fig. 7. Comparison of experimental and computational results for uniaxial tension boundary condition.

IV. CONCLUSION REMARKS

In the present study, detailed simulations on the mechanical behaviors of the nanocrystalline twinned Cu affected by twin/matrix lamellar microstructure geometry and grain size scale are performed by using the finite element method based on the CMSG theory. The main conclusions are obtained as followings:

(1) The characteristics of material microstructures have strong influence on the overall mechanical properties of the NCT material, and the occurrence of intergranular fracture is sensitive to the material microstructures.

(2) The overall mechanical behaviors (strength and ductility) of the NCT copper strongly depend on the grain boundary adhesion strength and interface fracture energy. Both overall strength and ductility of the NCT copper increase with the increasing of both the grain boundary adhesion strength and the interface fracture energy.

(3) The comparison between the results of numerical calculation and experimental data shows that the theory model adopted in the present research can well characterize the mechanical properties and size effect of NCT copper.

References

[1] Lu,L., Shen,Y.F., Chen,X.H., Qian,L. and Lu,K., Ultrahigh strength and high electrical conductivity in copper. *Science*, 2004, 304: 422-426.

[2] Shen,Y.F., Lu, L., Lu, Q.H., Jin,Z.H. and Lu,K., Tensile properties of copper with nano-scale twins. *Scripta Materialia*, 2005, 52: 989-994.

[3] Ma,E., Wang,Y.M., Lu,Q.H., Sui,M.L., Lu,L. and Lu,K., Strain hardening and large tensile elongation in ultrahigh-strength nano-twinned copper. *Applied Physics Letters*, 2004, 85: 4932-4934.

[4] Lu,L., Schwaiter,R., Shan,Z.W., Dao,M., Lu,K. and Suresh,S., Nano-sized twins induce high rate sensitivity of flow stress in pure copper. *Acta Materialia*, 2005, 53: 2169-2179.

[5] Jin,Z.H., Gumbsch,P., Ma,E., Albe,K., Lu,K., Hahn,H. and Gleiter,H., The interaction mechanism of screw dislocations with coherent twin boundaries in different face-centred cubic metals. *Scripta Materialia*, 2006, 54: 1163-1168.

[6] Zhu,T., Li,J., Samanta,A., Kim,H.G. and Suresh,S., Interfacial plasticity governs strain rate sensitivity and ductility in nanostructured metals. *Proceedings of the National Academy of Sciences*, 2007, 104: 3031-3036.

[7] Dao,M., Lu,L., Shen,Y.F. and Suresh,S., Strength, strain-rate sensitivity and ductility of copper with nanoscale twins. *Acta Materialia*, 2007, 54: 5421-5432.

[8] Schwaiger,R., Moser,B., Dao,M., Chollacoop,N. and Suresh,S., Some critical experiments on the strain-rate sensitivity of nanocrystalline nickel. *Acta Materialia*, 2003, 51: 5159-5172.

[9] Kumar,K.S., Van Swygenhoven,H. and Suresh,S., Mechanical behavior of nano-crystalline metals and alloys. *Acta Materialia*, 2003, 51: 5743-5774.

[10] Kumar,K.S., Suresh,S., Chisholm,M.F., Horton,J.A. and Wang,P., Deformation of electro- deposited nanocrystalline nickel. *Acta Materialia*, 2003, 51: 387-405.

[11] Han,C.S., Gao,H., Huang,Y. and Nix,W.D., Mechanism-based strain gradient crystal plasticity—I. Theory. *Journal of the Mechanics and Physics of Solids*, 2005, 53: 1188-1203.

[12] Han,C.S., Gao,H., Huang,Y. and Nix,W.D., Mechanism-based strain gradient crystal plasticity—II. Analysis. *Journal of the Mechanics and Physics of Solids*, 2005, 53: 1204-1222.

[13] Huang,Y., Qu,S., Hwang,K.C., Li,M. and Gao,H., A conventional theory of mechanism based strain gradient plasticity. *International Journal of Plasticity*, 2004, 20: 753-782.

[14] Qu,S., Huang,Y., Pharr,G.M. and Hwang, K.C., The indentation size effect in the spherical indentation of iridium: A study via the conventional theory of mechanism-based strain gradient plasticity. *International Journal of Plasticity*, 2006, 22: 1265-1286.

[15] Gao,H., Huang,Y., Nix,W.D. and Hutchinson,J.W., Mechanism-based strain gradient plasticity—I. Theory. *Journal of the Mechanics and Physics of Solids*, 1999, 47: 1239-1263.

[16] Qu,S., Huang,Y., Jiang, H., Liu,C., Wu,P.D. and Hwang,K.C., Fracture analysis in the conventional theory of mechanism-based strain gradient (CMSG) plasticity. *International Journal of Fracture*, 2004, 129: 199-220.

[17] Hibbit, Karlsson and Sorensen Inc. ABAQUS/Standard User's Manual Version 6.2, 2001.

[18] Barenblatt,G.I., The formation of equilibrium cracks during brittle fracture: general ideas and hypotheses, axially symmetric cracks. *Applied Mathematics and Mechanics*, 1959, 23: 622-636.

[19] Dugdale,D.S., Yielding of steel sheets containing slits. *Journal of the Mechanics and Physics of Solids*, 1960, 8: 100-104.

[20] Needleman,A., An analysis of tTensile decohesion along an interface. *Journal of the Mechanics and Physics of Solids*, 1990, 38: 289-324.
[21] Tvergaard,V. and Hutchinson,J.W., The relation between crack growth resistance and fracture process parameters in elastic-plastic solids. *Journal of the Mechanics and Physics of Solids*, 1992, 40: 1377-1397.
[22] Qu,S., Siegmund,T., Huang,Y., Wu,P.D., Zhang,F. and Hwang,K.C., A study of particle size effect and interface fracture in aluminum alloy composite via an extended conventional theory of mechanism-based strain-gradient plasticity. *Composites Science and Technology*, 2005, 65: 1244-1253.
[23] Warner,D.H. and Molinari,J.F., Micromechanical finite element modeling of compressive fracture in confined alumina ceramic. *Acta Materialia*, 2006, 54: 5135-5145.
[24] Van Swygenhoven,H. and Derlet, P.M., Grain-boundary sliding in nanocrystalline fcc metals. *Physical Review B*, 2001, 64: 1-9.
[25] Conrad,H. and Narayan,J., On the grain size softening in nanocrystalline materials. *Scripta Materialia*, 2000, 42: 1025-1030.
[26] Van der Sluis,O., Schreurs,P.J.G. and Meijer,H.E.H., Homogenization of structured elasto- viscoplastic solids at finite strains. *Mechanics of Materials*, 2001, 33: 499-522.
[27] Chen,X.H. and Lu,L., Work hardening of ultrafine-grained copper with nanoscale twins. *Scripta Materialia*, 2007, 57: 133-136.